The linear stability of oscillating pipe flow

C. Thomas,[1,a)] A. P. Bassom,[1,b)] and P. J. Blennerhassett[2]
[1]*School of Mathematics and Statistics, The University of Western Australia, Crawley, WA 6009, Australia*
[2]*School of Mathematics and Statistics, University of New South Wales, Sydney, NSW 2052, Australia*

(Received 4 May 2011; accepted 2 December 2011; published online 11 January 2012)

An investigation is made of the three-dimensional linear stability of the Stokes layer generated within a fluid contained inside a long oscillating cylinder. Both longitudinal and torsional vibrations are examined and the system of disturbance equations derived using Floquet theory are solved using pseudospectral methods. Critical parameters for instability are obtained for an extensive range of pipe radii and longitudinal and azimuthal wavenumbers. For sufficiently small pipe diameters, three-dimensional perturbations are sometimes found to be more unstable than their two-dimensional counterparts. In contrast, at larger radii, the three-dimensional disturbance modes are less important and the two-dimensional versions are expected to be observed in practice. These results imply constraints on experiments that are designed to exhibit shear modes in oscillatory flow. © *2012 American Institute of Physics*. [doi:10.1063/1.3675899]

I. INTRODUCTION

The archetype for many oscillatory flows is the planar Stokes layer, which develops in a semi-infinite layer of incompressible fluid when the bounding flat surface is driven back and forth in a sinusoidal manner. This time-periodic flow is one of the few exact solutions to the Navier-Stokes equations, making it an ideal choice for studying the disturbance characteristics of many unsteady flows.[1] Determining the stability of Stokes layers is not just a purely theoretical exercise for such motions can appear along the bounding surfaces of many high-frequency oscillating flows. As a simple example, at sufficiently large frequencies the oscillatory motion in channel and circular pipe flows may be divided into a uniform inner inviscid core plus Stokes layers at the wall(s).

Early theoretical investigators into the linear stability of the Stokes layer were based on Floquet theory analysis. Unfortunately these studies failed to locate any linearly unstable modes due to limitations imposed by the computational resources available. The investigation of Hall[2] revealed no evidence of instability for Reynolds numbers R (defined in Eq. (4) below) up to 160 and similarly, the results of von Kerczek and Davis[3] did not indicate the presence of growing disturbances for $R \leq 400$ in their study of the flow contained between an oscillating plate and a stationary wall. Only much later did Blennerhassett and Bassom[4] map out a portion of the linear stability neutral curve and predict a critical R of approximately 708 for the semi-infinite Stokes layer. Although this calculation of a neutral curve provided definitive evidence of a linear instability mode in Stokes layers, the associated critical conditions did not align with a large number of experimental studies.

There are various ways of setting up oscillatory layers in the laboratory. Depending on the precise configuration used, values of R between 140 and 270 have been suggested as the critical point when the laminar oscillatory flow becomes unstable.[5] It is noted these predictions are less than half of those calculated by Blennerhassett and Bassom[4] and various reasons for this discrepancy have been proposed. First, while the theoretical studies were conducted for a semi-infinite fluid, experimental investigations necessarily concern bounded flows and these are normally

[a)]Current address: Department of Mathematics, Imperial College, London SW7 2AZ, United Kingdom.
[b)]Electronic mail: Andrew.Bassom@uwa.edu.au.

contained within circular pipes. Clamen and Minton[6] generated Stokes layers by longitudinally oscillating a tube at a high frequency; other workers have used a stationary pipe with a piston that drives oscillatory motion in the fluid.[5,7–10] In order to account for these confined geometries Blennerhassett and Bassom[11] extended their investigation of oscillatory flow in a semi-infinite layer to the stability of shear modes within channels and axisymmetric shear modes in circular pipes. The critical value of R was lowered to about 570 for a pipe of radius roughly 10 Stokes layer thicknesses and so, although the introduction of curvature brings the theoretical work nearer the practical findings, a rather large discrepancy remains.

Wall imperfections or other external forces have also been proposed as explanations for the disagreements between theory and experiment,[12–16] as external noise may trigger premature instability and turbulence in oscillatory flow experiments. Alternatively, it has been suggested that in the presence of moderate to relatively high level disturbances transition may not be associated with linear Floquet instability at all but is either a strictly nonlinear phenomenon or arises after a linear instantaneous growth followed by nonlinear development.[16,17] While not the focus of the present work, there has also been extensive investigation into the relevance of Floquet instability modes in time periodic flows in those cases where there is an underlying non-zero mean forcing.[18–20] For slowly varying forcing it was shown that external noise coupled with weakly nonlinear effects could lead to a flow which was not periodic in time.[19,20]

Blennerhassett and Bassom[21] suggested that the external noise due to an oscillating piston within a long pipe may be reduced, or even completely eliminated, by instead considering the flow contained within a cylinder oscillating about its longitudinal axis. It would be expected that as the radius of the cylinder grows so the basic flow asymptotes towards the flat Stokes layer as curvature effects become negligible. However, this curvature now makes the flow prone to axially periodic vortices, generated by centripetal effects.[22] Thus the suggested basic flow now admits two distinct modes of instability: shear modes associated with the planar Stokes layer and vortex modes associated with the curved geometry. Further, both of these disturbance modes could be fully three-dimensional, making it potentially difficult to design experimental apparatus to detect the planar Stokes shear mode. Initially, both axisymmetric vortices and two-dimensional shear modes were considered[21] in an attempt to predict the range of cylinder radii for which the dominant type of instability is the Stokes layer shear mode. This calculation was motivated by the desire to know whether the observation of shear modes in a fluid within a torsionally oscillating cylinder would require apparatus of an impractical size. Based on some arbitrary assumptions for experimental conditions the results suggested that a cylinder of radius in the order of 40 cm could be used.[21] However, it should be noted that it was not the cross-over from centripetal to shear mode instabilities that determined the size of the needed apparatus, but rather the requirement to attain Reynolds numbers around the critical value of approximately 708.

As yet a laboratory experiment of the type envisaged in Ref. 21 has not been performed, and before such a task is contemplated the possible role of three-dimensional disturbances needs to be determined. The computational methods employed for the longitudinally vibrating cylinder[11] and for the torsional problem[21] meant that only two-dimensional perturbations were investigated in these papers. Such a simplification can be justified rigorously for the linear stability of the flat Stokes layer or of the oscillatory flow in a channel because in these geometries Squire's theorem can be shown to hold.[3,23] However, an equivalent result can not be deduced for the case of a cylindrical pipe. A complete investigation of the linear stability of this problem must therefore allow for a fully three-dimensional disturbance and this is the objective of the remainder of this paper. There is the real possibility that three-dimensionality may significantly modify the conclusions of Refs. 11 and 21.

Our study is organised as follows. In Sec. II, we develop in parallel the governing equations for both basic flows and describe the pseudospectral methods implemented for the computations. Critical parameters for instability are presented in Sec. III for both longitudinal and torsional flows and some discussion is given in Sec. IV.

II. FORMULATION

Our concern is with an incompressible viscous fluid contained within a long circular pipe which oscillates with angular frequency ω. In due course we shall be interested in the two separate

problems of longitudinal oscillations, when the vibration is parallel to the axis of the cylinder, and with torsional oscillations, when the motion is about the axis. Rather than develop these two cases separately it is convenient to consider a composite in which the cylinder is permitted to move both parallel to its axis with velocity $U_0 \cos \omega t$ and about it with velocity $W_0 \cos \omega t$; it is obvious that purely longitudinal or torsional oscillations are obtained by setting $W_0 = 0$ or $U_0 = 0$, respectively.

The motion then induced in the fluid is best described relative to standard cylindrical coordinates (x, r, θ) in which all lengths have been made dimensionless by scaling on the Stokes layer thickness $\sqrt{2\nu/\omega}$ where ν denotes the kinematic viscosity of the fluid. It is supposed that in these units the cylinder is of radius $r = H$ and if the velocities are scaled on either U_0 or W_0 as appropriate and time is scaled according to $\tau = \omega t$, then the undisturbed basic flow is given by

$$U_B(r, \tau) = \{U, 0, W\}, \tag{1a}$$

where

$$U = \Re\left(\frac{J_0((1-i)r)}{J_0((1-i)H)}\exp\{i\tau\}\right) = u_1 e^{i\tau} + u_{-1}e^{-i\tau}, \qquad W = 0, \tag{1b}$$

for longitudinal flow, while

$$U = 0, \qquad W = \Re\left(\frac{J_1((1-i)r)}{J_1((1-i)H)}\exp\{i\tau\}\right) = w_1 e^{i\tau} + w_{-1}e^{-i\tau}, \tag{1c}$$

for torsional flow. In these expressions J_0 and J_1 denote the usual zeroth and first order Bessel functions, and $\Re$ denotes the real part.

The basic flow is disturbed so that the velocity components are $U_B + \varepsilon\{f, g, h\}$ and the corresponding pressure field is perturbed by εp. If these expressions are substituted into the three-dimensional Navier-Stokes and continuity equations and linearised in ε then the resulting governing equations are

$$\frac{\partial f}{\partial \tau} + R_L\left(U\frac{\partial f}{\partial x} + g\frac{\partial U}{\partial r}\right) + \frac{R_T}{r}\frac{\partial f}{\partial \theta}W = -\frac{\partial p}{\partial x} + \frac{1}{2}\nabla^2 f, \tag{2a}$$

$$\frac{\partial g}{\partial \tau} + R_L U\frac{\partial g}{\partial x} + \frac{R_T W}{r}\left(\frac{\partial g}{\partial \theta} - 2h\right) = -\frac{\partial p}{\partial r} + \frac{1}{2}\left[\nabla^2 g - \frac{g}{r^2} - \frac{2}{r^2}\frac{\partial h}{\partial \theta}\right], \tag{2b}$$

$$\frac{\partial h}{\partial \tau} + R_L U\frac{\partial h}{\partial x} + R_T\left\{g\frac{\partial W}{\partial r} + \frac{W}{r}\left(\frac{\partial h}{\partial \theta} + g\right)\right\} = -\frac{1}{r}\frac{\partial p}{\partial \theta} + \frac{1}{2}\left[\nabla^2 h - \frac{h}{r^2} + \frac{2}{r^2}\frac{\partial g}{\partial \theta}\right], \tag{2c}$$

$$\frac{\partial f}{\partial x} + \frac{1}{r}\frac{\partial (rg)}{\partial r} + \frac{1}{r}\frac{\partial h}{\partial \theta} = 0, \tag{2d}$$

where

$$\nabla^2 = \frac{\partial^2}{\partial x^2} + \frac{1}{r}\frac{\partial}{\partial r}\left(r\frac{\partial}{\partial r}\right) + \frac{1}{r^2}\frac{\partial^2}{\partial \theta^2}. \tag{3}$$

In these equations the Reynolds numbers for the respective longitudinal and torsional motions are given by

$$R_L = \frac{U_0}{\sqrt{2\nu\omega}} \quad \text{and} \quad R_T = \frac{W_0}{\sqrt{2\nu\omega}}. \tag{4}$$

In order to investigate the stability of the flow to three-dimensional perturbations, the velocity components f, g, and h and the pressure p were expressed in the forms,

$$\{f, g, h, p\}(x, r, \theta, \tau) = \{\tilde{f}, \tilde{g}, \tilde{h}, \tilde{p}\}(r, \tau)\exp\{\mu\tau + iax + iq\theta\} + \text{complex conjugate}, \tag{5}$$

where a is the real wavenumber in the x-direction, q is the integer-valued azimuthal wavenumber and functions designated $\sim$ are all 2π-periodic in τ. Here any temporal growth or decay in the disturbance is contained within the complex Floquet exponent μ. This decomposition does not define

μ uniquely but symmetry arguments show that its imaginary part μ_i can be taken to lie within the range $[0, 0.5]$ without loss of generality.

These expressions now yield an eigenvalue computational problem for μ given specified values of a, q, and the Reynolds number. Rather than tackling the system written in terms of primitive variables, we take advantage of the observation of Burridge and Drazin[24] that it is convenient to define the new quantities,

$$\phi = -ir\tilde{g} \qquad \text{and} \qquad \Omega = \frac{ar\tilde{h} - q\tilde{f}}{l^2} \qquad \text{where} \quad l^2 = a^2r^2 + q^2. \tag{6}$$

If differential operators S and T are given by

$$S = \frac{\partial^2}{\partial r^2} + \frac{(3a^2r^2 + q^2)}{rl^2}\frac{\partial}{\partial r} - \frac{l^2}{r^2} \quad \text{and} \quad T = \frac{\partial^2}{\partial r^2} + \frac{(q^2 - a^2r^2)}{rl^2}\frac{\partial}{\partial r} - \frac{l^2}{r^2}, \tag{7}$$

then the governing system (2) may be cast as

$$\begin{aligned}
&\begin{bmatrix} T(\mu + \partial_\tau) & 0 \\ 0 & \mu + \partial_\tau \end{bmatrix}\begin{bmatrix} \phi \\ \Omega \end{bmatrix} + iaR_L\begin{bmatrix} UT - (l^2/r)(rU'/l^2)' & 0 \\ -qU'/(al^2r) & U \end{bmatrix}\begin{bmatrix} \phi \\ \Omega \end{bmatrix} \\
&\quad + \frac{iqR_T}{r}\begin{bmatrix} WT - (l^2/r)\left\{(rW'/l^2)' - W\left((1/rl^2) - (1/l^2)'\right)\right\} & -2aWl^2/q \\ a(rW)'/ql^2 & W \end{bmatrix}\begin{bmatrix} \phi \\ \Omega \end{bmatrix} \\
&\quad = \frac{1}{2}\begin{bmatrix} T^2 & -2aqT \\ (2aq/l^4)T & S \end{bmatrix}\begin{bmatrix} \phi \\ \Omega \end{bmatrix},
\end{aligned} \tag{8}$$

where a prime denotes differentiation with respect to r. This system needs to be solved subject to suitable regularity conditions on the axis of the pipe $r = 0$ together with the requirement that the three perturbation quantities f, g, and h all vanish on the pipe wall $r = H$. Expressed in terms of the computational variables this necessitates that

$$\phi = \phi' = \Omega = 0 \text{ on } r = H. \tag{9}$$

In view of the decomposition (Eq. (5)) the unknowns ϕ and Ω are 2π-periodic in time τ and so have the Fourier decompositions,

$$\{\phi, \Omega\} = \sum_{n=-\infty}^{n=\infty} \{\phi_n(r), \Omega_n(r)\}\exp(in\tau). \tag{10}$$

The comparison of harmonics in Eq. (8) then leads to the infinite system of coupled ordinary differential equations,

$$\begin{aligned}
(T/2 - \mu - in)T\phi_n - aqT\Omega_n = {} & iaR_L[(u_1T - u_{1,L})\phi_{n-1} + (u_{-1}T - u_{-1,L})\phi_{n+1}] \\
& + \frac{iqR_T}{r}[(w_1T - w_{1,L})\phi_{n-1} + (w_{-1}T - w_{-1,L})\phi_{n+1}] \\
& - \frac{2ial^2R_T}{r}[w_1\Omega_{n-1} + w_{-1}\Omega_{n+1}],
\end{aligned} \tag{11a}$$

$$\begin{aligned}
\frac{aq}{l^4}T\phi_n + (S/2 - \mu - in)\Omega_n = {} & -\frac{iqR_L}{rl^2}[u_1'\phi_{n-1} + u_{-1}'\phi_{n+1}] \\
& + \frac{iaR_T}{rl^2}[(rw_1)'\phi_{n-1} + (rw_{-1})'\phi_{n+1}] \\
& + iaR_L[u_1\Omega_{n-1} + u_{-1}\Omega_{n+1}] \\
& + \frac{iqR_T}{r}[w_1\Omega_{n-1} + w_{-1}\Omega_{n+1}],
\end{aligned} \tag{11b}$$

in which the quantities,

$$u_{1,L} = i\frac{J_0((1-i)r)}{J_0((1-i)H)} + \frac{(1-i)a^2 r}{l^2}\frac{J_1((1-i)r)}{J_0((1-i)H)} \tag{12a}$$

and

$$w_{1,L} = i\frac{J_1((1-i)r)}{J_1((1-i)H)} - \frac{(1-i)a^2 r}{l^2}\frac{J_0((1-i)r)}{J_1((1-i)H)}. \tag{12b}$$

Note that $u_{1,L}$ in Eq. (12a) can be reformulated, using the properties of Bessel functions, to bring it to a form analogous to that given in Ref. 11.

A. Numerical methods

The system (11) was solved numerically using the pseudospectral techniques described by Fornberg[25] and Trefethen.[26] The differential operators appearing in Eq. (11) were replaced by appropriate pseudospectral matrix approximations and each $\{\phi_n(r), \Omega_n(r)\}$ represented as a vector $\{\boldsymbol{\phi}_n, \boldsymbol{\Omega}_n\}$ of function values on a Chebyshev mesh over the interval $0 \le r \le H$. If the matrix operators

$$\begin{aligned} &\mathbf{M}_L = \mathbf{T^{-1}}(u_1\mathbf{T} - u_{1,L}\mathbf{I}), \quad \mathbf{M}_T = \mathbf{T^{-1}}r^{-1}(w_1\mathbf{T} - w_{1,L}\mathbf{I}), \quad \mathbf{K}_T = \mathbf{T^{-1}}r^{-1}l^2 w_1\mathbf{I}, \\ &\mathbf{P}_L = (rl^2)^{-1}u_1'\mathbf{I}, \quad \mathbf{P}_T = (rl^2)^{-1}(rw_1)'\mathbf{I}, \quad \mathbf{Q}_L = u_1\mathbf{I}, \quad \mathbf{Q}_T = r^{-1}w_1\mathbf{I}, \end{aligned} \tag{13}$$

are introduced, where $\mathbf{I}$ is the identity matrix, and if the differential operators S and T are replaced by the matrices $\mathbf{S}$ and $\mathbf{T}$, respectively, then Eq. (11) becomes

$$\begin{aligned} &-i(aR_L\widetilde{\mathbf{M}}_L + qR_T\widetilde{\mathbf{M}}_T)\boldsymbol{\phi}_{\mathbf{n+1}} + (\mathbf{T^{-1}T^2}/2 - in\mathbf{I})\boldsymbol{\phi}_{\mathbf{n}} - i(aR_L\mathbf{M}_L + qR_T\mathbf{M}_T)\boldsymbol{\phi}_{\mathbf{n-1}} \\ &\quad + 2iaR_T\widetilde{\mathbf{K}}_T\Omega_{\mathbf{n+1}} - aq\mathbf{I}\Omega_{\mathbf{n}} + 2iaR_T\mathbf{K}_T\Omega_{\mathbf{n-1}} = \mu\boldsymbol{\phi}_{\mathbf{n}}, \end{aligned} \tag{14a}$$

$$\begin{aligned} &-i(aR_L\widetilde{\mathbf{Q}}_L + qR_T\widetilde{\mathbf{Q}}_T)\Omega_{\mathbf{n+1}} + (\mathbf{S}/2 - in\mathbf{I})\Omega_{\mathbf{n}} - i(aR_L\mathbf{Q}_L + qR_T\mathbf{Q}_T)\Omega_{\mathbf{n-1}} \\ &\quad i(qR_L\widetilde{\mathbf{P}}_L - aR_T\widetilde{\mathbf{P}}_T)\boldsymbol{\phi}_{\mathbf{n+1}} + \frac{aq}{l^4}\mathbf{T}\boldsymbol{\phi}_{\mathbf{n}} + i(qR_L\mathbf{P}_L - aR_T\mathbf{P}_T)\boldsymbol{\phi}_{\mathbf{n-1}} = \mu\Omega_{\mathbf{n}}. \end{aligned} \tag{14b}$$

In this definition a $\sim$ represents the complex conjugate of the corresponding matrix.

A finite system of equations was obtained by truncating the Fourier series Eq. (10) for $\{\phi, \Omega\}$ and then setting $\boldsymbol{\phi}_n = \Omega_n = 0$ for all $|n| > N$. The system of equations (14) could then be cast as the algebraic eigenvalue problem,

$$\mathbf{A}\boldsymbol{\Phi} = \mu\boldsymbol{\Phi}, \tag{15}$$

in which $\mathbf{A}$ is a sparse matrix and the vector $\boldsymbol{\Phi}$ is given by

$$\boldsymbol{\Phi}^T = (\boldsymbol{\phi}_N^T\boldsymbol{\phi}_{N-1}^T \ldots \boldsymbol{\phi}_0^T \ldots \boldsymbol{\phi}_{-N}^T \quad \Omega_N^T\Omega_{N-1}^T \ldots \Omega_0^T \ldots \Omega_{-N}^T). \tag{16}$$

The eigenvalues μ and eigenvectors $\boldsymbol{\Phi}$ were obtained using the sparse matrix eigenvalue routines available in MATLAB. Checks on the consistency and accuracy of μ and $\boldsymbol{\Phi}$ were conducted, similar to those outlined in the studies of Refs. 11 and 21. Empirically it was found that eigenvalues were accurately determined provided that the Chebyshev domain $0 \le r \le H$ was divided into at least 100 intervals and the number of harmonics N was at least $0.8aR_L$ or $0.8qR_T/H$ for the longitudinal and torsional flow problems, respectively.

III. RESULTS

A. Longitudinal flow

The first set of calculations relate to the case when the pipe oscillates longitudinally with the basic velocity profile given by Eq. (1b). For a prescribed pipe radius H and azimuthal disturbance wavenumber q, the Reynolds number R_L for instability was found as a function of the streamwise wavenumber a; its critical value $R_{L,c}$ could then be estimated. One view of the results appears in Fig. 1(a) which shows how $R_{L,c}$ varies as a function of H for various fixed q. It is noted that as H

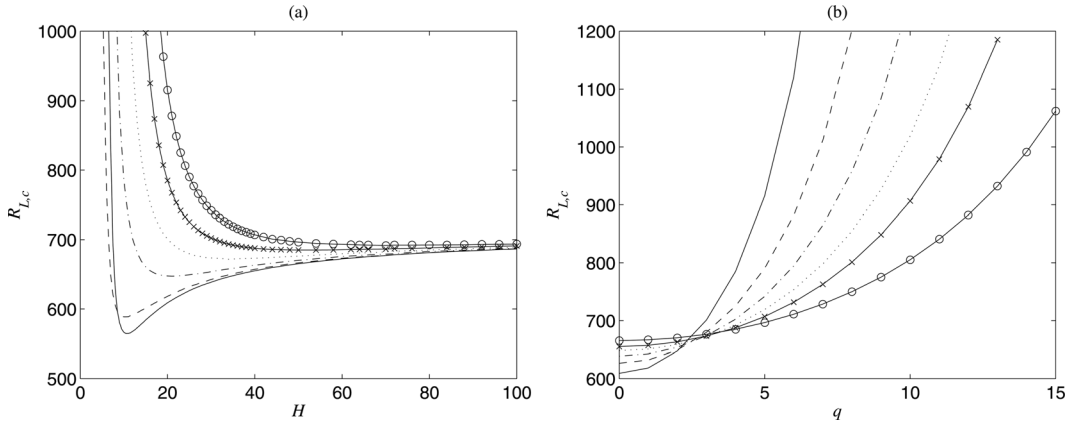

FIG. 1. (a): Critical Reynolds number $R_{L,c}$ as a function of dimensionless pipe radius H for azimuthal wavenumbers $q = 0$ (solid line), $q = 1$ (dashed lines), $q = 2$ (chain line), $q = 3$ (dotted line), $q = 4$ (solid-crossed line) and $q = 5$ (solid-circle line). (b) $R_{L,c}$ against q for $H = 20$ (solid line), $H = 25$ (dashed line), $H = 30$ (chain line), $H = 35$ (dotted line), $H = 40$ (solid-crossed line) and $H = 50$ (solid-circle line).

increases all the modes approach the common limiting value of approximately 708, the critical Reynolds number for instability of a planar Stokes layer. In passing we note that the numerical results suggest that $R_{L,c} - 708 \sim O(H^{-1})$, in keeping with expectations for the transition from a cylindrical geometry to a planar one as $H \to \infty$. A more complicated version of this $O(H^{-1})$ decay to planar results is seen in the results for shear instability modes in a torsionally oscillating cylinder, described in Sec. III B. The figure also demonstrates that $R_{L,c}$ for axisymmetric ($q = 0$) disturbances is smallest (approximately 564) when the pipe radius $H \approx 11$, in agreement with previous conclusions.[11] Apart from quite small H it appears that $R_{L,c}$ increases monotonically with q and it is only when $H \leq 8.5$ that a more complicated behaviour occurs. Then, for these smaller values of H and the range of R_L considered here, the most dangerous mode is that with $q = 1$. It can be concluded that in a longitudinally oscillating pipe of sufficiently large radius it is the two-dimensional disturbance modes of Ref. 11 that are likely to be the most prominent. Fig. 1(b) confirms this supposition; here the critical $R_{L,c}$ is shown as a function of the azimuthal wave number for several pipe radii in the range $20 \leq H \leq 50$. (We remark that the necessarily discrete data points in this graph have been joined by straight lines to aid the identification of results at fixed values of H.) We see that the points $(q, R_{L,c})$, for a given H, appear to lie on a roughly parabolic concave-up shaped curve, and for this range of H, the curve containing the smallest value of $R_{L,c}$ corresponds to the two-dimensional disturbances with $q = 0$.

B. Torsional flow

The results obtained here for the linear stability of the torsional base flow given by Eq. (1c) are an extension of those presented in Ref. 21. Of interest is the value of R_T for neutrally stable disturbances as a function of the parameters q, a, and H, which is here denoted $R_{T,N}(q, a, H)$. The results of Ref. 21 thus correspond to our results for $R_{T,N}(q, 0, H)$, and these are represented by the solid lines in Fig. 2. The agreement between the current results with $a = 0$ and previous results[21] is extremely good, with neutral conditions consistent to five or more significant figures. More precisely, what is plotted in Fig. 2 are the critical Reynolds numbers for instability for even integer (labelled by $\times$) and odd integer (labelled by $\bigcirc$) wavenumbers q, defined as

$$R_{T,c} = \min_{k \in Z} R_{T,N}(2k, a, H),$$

for even values of q with a similar definition holding for odd values of q.

The structure of the curves for $a = 0$ in Fig. 2 is rather complicated, and the interested reader is referred to Ref. 21 for a full discussion, but some of the key ideas can at least be summarised here. Complete neutral stability curves $R_{T,N}(q, 0, H)$ can be constructed for each fixed integer q; as q increases so the characteristic parabolic-like shape of the curve shifts to the right of the figure

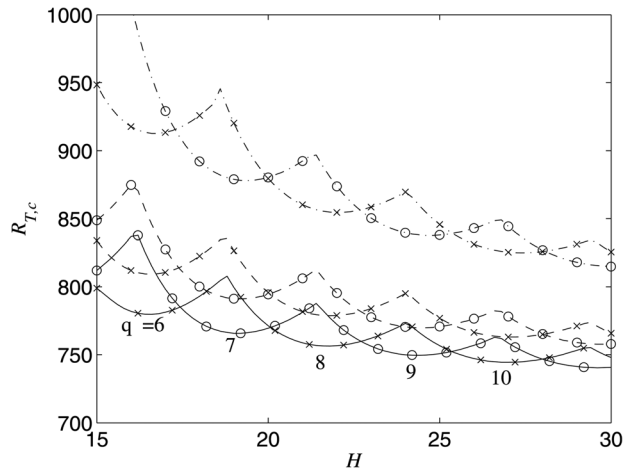

FIG. 2. Even (×) and odd (○) integer wavenumber critical conditions $R_{T,c}$ as a function of H, for wavenumbers $a = 0$ (solid lines), $a = 0.05$ (dashed lines) and $a = 0.1$ (chain lines).

towards higher values of H and the corresponding Reynolds numbers slightly drops. What is shown in Fig. 2 for $a = 0$ are the lowermost parts of the neutral curves for the integer values of $q \in [6, 10]$. The interpretation of these results is that when $a = 0$ and $H = 15$ the preferred azimuthal wavenumber is $q = 6$ and as the pipe widens so this most dangerous mode shifts progressively to larger q. This is to be expected when it is remembered that as $H \to \infty$ curvature effects become weaker and the flow increasingly mimics a flat Stokes layer. Then it is of no surprise that the ratio q/H approaches 0.38, the critical wavenumber for linear instability in the planar Stokes layer[4] and hence the critical azimuthal wavenumber $q \sim 0.38H$. It is this phenomenon that leads to an overlapping of the curves $R_{T,N}(q, a, H)$ for fixed q and a as the pipe radius H increases which in turn is responsible for the "sawtooth" curve profiles seen in Fig. 2.

Superimposed on the $a = 0$ results in Fig. 2 are curves for $R_{T,N}$ corresponding to the two wavenumbers $a = 0.05$ and $a = 0.1$. It is clear that for these wave numbers three-dimensional disturbances are more stable than their two-dimensional counterparts. Thus it appears that the previous calculations[21] did delineate the most important shear modes in the torsionally oscillating cylinder geometry. However, as mentioned in Sec. I, one important consideration explored in Ref. 21 was the competition between shear and centripetal disturbance modes. With the current, more general formulation of the linear stability problem, the previous results[21] for two-dimensional (axisymmetric) vortex modes can now be extended to fully three-dimensional centripetal instabilities. The governing equations for centripetal disturbance modes are automatically contained within Eqs. (8) and (14) with the basic flow taken to be Eq. (1c). Here the critical Reynolds number for instability, $R_{T,c}$ as a function of q and H, is defined as

$$R_{T,c} = \min_{a \in R} R_{T,N}(q, a, H)$$

and values of $R_{T,c}$ for various non-axisymmetric centripetal instabilities are plotted in Fig. 3 for H in the range $8 \le H \le 144$. Disturbances with azimuthal wavenumber $q \le 5$ were investigated and, at least for the range of H considered, some of the non-axisymmetric disturbances appear at lower Reynolds numbers than the axisymmetric $q = 0$ disturbances (solid line). Rounding the values of H to integers we find that for radius $8 \le H \le 16$, the $q = 1$ instability appears first and then as H increases the preferred azimuthal wavenumber grows in concert so that $q = 2$ is the dominant mode for $H \in [16, 44]$, $q = 3$ for $H \in [44, 86]$, and $q = 4$ when $H \in [86, 144]$. Further calculations indicate that this behaviour persists for larger values of H. We note in passing that the axial wavenumber a at critical conditions is only weakly dependent on H, tending to a constant dependent on q as H becomes large. When $q = 0$ the wavenumber at critical conditions tends to 1.915… (Ref. 21) as H increases, while for $q = 4$ the corresponding critical wavenumber is approximately 1.6 for $H \gtrsim 65$. For $q > 4$, the axial wavenumber at critical conditions increases slowly with increasing q.

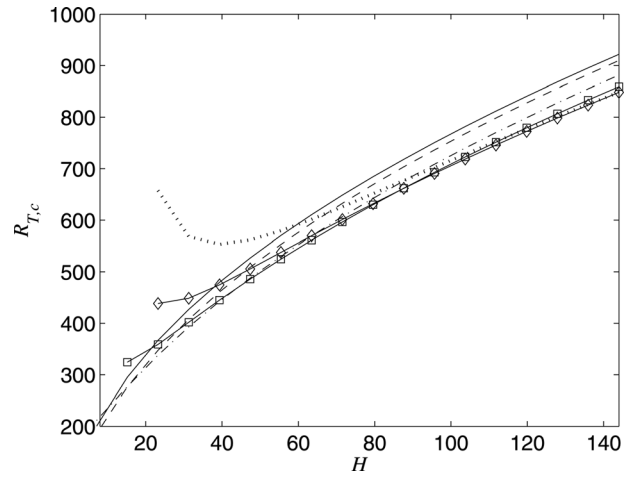

FIG. 3. Critical Reynolds number $R_{T,c}$ for non-axisymmetric centripetal disturbances as a function of dimensionless pipe radius H for azimuthal wavenumbers $q = 0$ (solid line), $q = 1$ (dashed lines), $q = 2$ (chain line), $q = 3$ (solid-square line), $q = 4$ (solid-diamond line) and $q = 5$ (dotted line).

Although some of the three-dimensional centripetal modes are more unstable than their two-dimensional counterparts, their respective critical Reynolds numbers increase with H. It has already been noted that the shear instability, $a = 0$, appears at a value of $R_{T,c}$ which tends to the flat Stokes layer value of 708 as $H \to \infty$. Thus there must be a cross-over value of H at which the three-dimensional centripetal modes and the shear instability are equally unstable. In Fig. 4 is shown the critical Reynolds numbers for the centripetal modes (crosses) plotted as functions of q for pipe radii $H = 88$, 96, 104, and 112. The necessarily discrete results for these critical conditions have been linked by a dotted line in this figure to accentuate the behaviour of these critical conditions as a function of the discrete azimuthal wavenumber q. The dashed lines in Fig. 4 delineate the Reynolds number values at which the two-dimensional shear mode first becomes unstable. For all the values of H taken, it is the $q = 4$ centripetal mode which is the first to become unstable and for the smaller two values of H shown it appears before the shear mode. On the other hand,

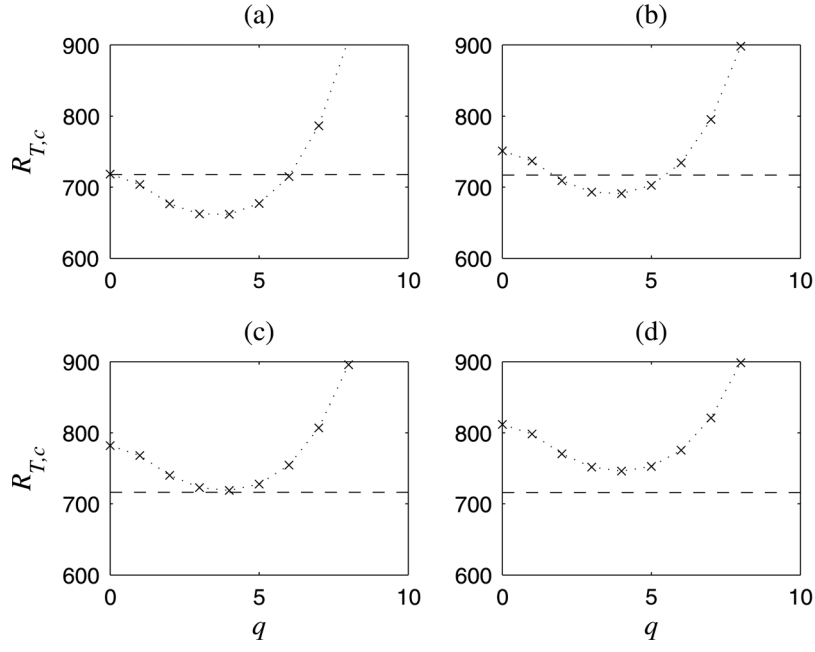

FIG. 4. Critical Reynolds number $R_{T,c}$ for instability to centripetal modes (crosses) as a function of the azimuthal wavenumber q, for (a) $H = 88$, (b) $H = 96$, (c) $H = 104$ and (d) $H = 112$. The horizontal dashed line indicates the critical R_T for the Stokes layer shear mode instability at the given value of H. This shear mode has $a = 0$ and $q \approx 0.38H$.

once $H = 104$ the centripetal and shear instabilities have almost identical neutral conditions ($R_{T,c} \approx 716$). Thus, this value of H corresponds to the location where the two disturbances swap over and for all greater pipe radii it is the shear mode which is the more unstable. This is further emphasised by the critical conditions at $H = 112$ (Fig. 4(d)) where the centripetal neutral curve has shifted up the $R_{T,c}$ axis.

IV. DISCUSSION

Here the focus has been on assessing how three-dimensionality affects the stability of longitudinally and torsionally oscillating cylinder flows. For the case of the longitudinal oscillations it has been found that the most unstable modes are actually two-dimensional, at least for cylinder radii greater than $H \approx 8.5$. Non-axisymmetric disturbances are technically the favoured mode of instability for smaller radii, but such radii are not particularly relevant to experimental simulations of planar Stokes layers, as in such investigations the pipe radius is chosen to minimise the curvature effects which are obviously absent in the planar Stokes layer. Thus, for linear instability, three-dimensionality is an unlikely explanation of the discrepancy between theoretical predictions and experimental determinations of the critical Reynolds number for instability of the Stokes layer.

The effects of three-dimensionality on the Stokes shear mode in the torsionally oscillating problem were also found to be insignificant, as the two-dimensional disturbance remains the most unstable. This result is entirely consistent with the conclusions in the previously discussed case of longitudinal oscillations, as the shear modes in the torsionally oscillating flow are the analogues of the shear modes discussed above. However, as the centripetal modes are destabilized by three-dimensional effects, we must revisit the proposal[21] that a torsionally vibrating cylinder could provide a practical apparatus capable of locating critical conditions for the instability of essentially planar Stokes layers.

The results presented here indicate that a cylinder of radius at least 104 Stokes layer thicknesses would be required in order to ensure that shear mode instabilities appear before any centripetal disturbances. This condition is slightly stronger than that given in Ref. 21, but this new result does not imply that experimental apparatus physically larger than previously predicted[21] is required. For a given working fluid, frequency and amplitude of oscillation, it was shown[21] that it was the achievement of Reynolds numbers around critical, say approximately 710, that controlled the physical properties of any experimental equipment. If Θ is used to denote the angular amplitude of oscillation of the cylinder, then the Reynolds number R_T can be rewritten as $R_T = H\Theta$. To guarantee that Stokes layer shear modes are the first instability to occur, we can now safely assume a value of H of say 120 and then vary the value of Θ to obtain values of R_T needed for instability. Using water as the working fluid, with a frequency of oscillation of 1 Hz,[21] this value of H leads to a cylinder with a dimensional radius of $120 \times 5.6 \times 10^{-1} \approx 70$ mm. This estimate of the physical size of the experimental equipment is much smaller than the very conservative estimates made previously.[21]

Finally, we point out that the linear stability equations (8) cover more problems than those reported on here and in particular we are not restricted to separate longitudinal or torsional oscillations. By using a velocity scaling of $\sqrt{2\nu\omega}$, rather than U_0 or W_0 as done originally, the undisturbed velocity field can be written,

$$U_B(r, \tau) = \{R_L U, 0, R_T W\},$$

with U given by Eq. (1b) and W given by Eq. (1c). For non-zero values of both R_L and R_T, the base flow is now two-dimensional with its linear stability still governed by Eq. (8). It is also possible to consider a more general motion for the bounding cylinder. As an example, changing the azimuthal wall velocity from $W_0 \cos \omega t$ to $W_0 \sin \omega t$ produces a basic flow which is the cylindrical geometry analogue of the orbital plate problem.[27] This example also demonstrates the need for a third parameter to define the phase relationship between the longitudinal and torsional oscillations, hence pointing to a much larger parameter space for any stability investigations. However, as the results in Ref. 27 indicated that the planar two-dimensional basic flow was

more unstable than its three-dimensional counterpart, similar results in the cylindrical geometry could be anticipated.

ACKNOWLEDGMENTS

We thank the referees for their helpful comments on this paper. This work was supported by the Australian Research Council by grant DP0880463.

[1]S. H. Davis, "The stability of time-periodic flows," Annu. Rev. Fluid Mech. **8**, 57 (1976).
[2]P. Hall, "The linear stability of flat Stokes layers," Proc. R. Soc. London A **359**, 151 (1978).
[3]C. von Kerczek and S. H. Davis, "Linear stability theory of oscillatory Stokes layers," J. Fluid Mech. **62**, 753 (1974).
[4]P. J. Blennerhassett and A. P. Bassom, "The linear stability of flat Stokes layers," J. Fluid Mech. **464**, 393 (2002).
[5]R. Akhavan, R. D. Kamm, and A. H. Shapiro, "An investigation of transition to turbulence in bounded oscillatory Stokes flows. Part 1. Experiments," J. Fluid Mech. **225**, 395 (1991).
[6]M. Clamen and P. Minton, "An experimental investigation of flow in an oscillatory pipe," J. Fluid Mech. **77**, 421 (1977).
[7]P. Merkli and H. Thomann, "Transition to turbulence in oscillating pipe flow," J. Fluid Mech. **68**, 567 (1975).
[8]M. Hino, M. Sawamoto, and S. Takasu, "Experiments on transition to turbulence in an oscillatory pipe flow," J. Fluid Mech. **75**, 193 (1976).
[9]D. M. Eckmann and J. B. Grotberg, "Experiments on transition to turbulence in oscillatory pipe flow," J. Fluid Mech. **222**, 329 (1991).
[10]C. R. Lodahl, B. M. Sumer, and J. Fredsøe, "Turbulent combined oscillatory flow and current in a pipe," J. Fluid Mech. **373**, 313 (1998).
[11]P. J. Blennerhassett and A. P. Bassom, "The linear stability of high-frequency oscillatory flow in a channel," J. Fluid Mech. **556**, 1 (2006).
[12]P. Blondeaux and G. Vittori, "Wall imperfections as a triggering mechanism for Stokes-layer transition," J. Fluid Mech. **67**, 107 (1994).
[13]R. Verzicco and G. Vittori, "Direct simulation of transition in Stokes boundary layers," Phys. Fluids **8**, 1341 (1996).
[14]G. Vittori and R. Verzicco, "Direct simulation of transition in an oscillatory boundary layer," J. Fluid Mech. **371**, 207 (1998).
[15]R. Tuzi and P. Blondeaux, "Intermittent turbulence in a pulsating pipe flow," J. Fluid Mech. **599**, 51 (2008).
[16]J. Luo and X. Wu, "On the linear stability of a finite Stokes layer: instantaneous versus Floquet modes," Phys. Fluids **22**, 054106 (2010).
[17]X. Wu and S. J. Cowley, "On the nonlinear evolution of instability modes in unsteady shear layers: the Stokes layer as a paradigm," Q. J. Mech. Appl. Math. **48**, 159 (1995).
[18]S. Rosenblat, "Centrifugal instability of time-dependent flows. Part 1. Inviscid, periodic flows," J. Fluid Mech. **33**, 321 (1968).
[19]R. Finucane and R. Kelly, "Onset of instability in a fluid layer heated sinusoidally from below," Int. J. Heat Mass Transfer **19**, 71 (1976).
[20]P. Hall, "On the nonlinear stability of slowly varying time-dependent viscous flows," J. Fluid Mech. **126**, 357 (1983).
[21]P. J. Blennerhassett and A. P. Bassom, "The linear stability of high-frequency flow in a torsionally oscillating cylinder," J. Fluid Mech. **576**, 491 (2007).
[22]D. Papageorgiou, "Stability of unsteady viscous flow in a curved pipe," J. Fluid Mech. **182**, 209 (1987).
[23]P. W. Conrad and W. O. Criminale, "The stability of time-dependent laminar flow: parallel flows," Z. Agnew. Math. Phys. **16**, 233–254 (1965).
[24]D. Burridge and P. Drazin, "Comments on 'stability of pipe Poiseuille flow'," Phys. Fluids **12**(1), 264 (1969).
[25]B. Fornberg, *A Practical Guide to Pseudospectral Methods* (Cambridge University Press, Cambridge, U.K., 1996).
[26]L. N. Trefethen, *Spectral methods in MATLAB* (SIAM, Philadelphia, PA, 2000).
[27]P. J. Blennerhassett and A. P. Bassom, "A note on the linear stability of a two-dimensional Stokes layer," Q. J. Mech. Appl. Math. **60**, 391 (2007).